

Article

## Characterization of Novel Castor Oil-Based Polyurethane Polymer Electrolytes

Salmiah Ibrahim <sup>1,\*</sup>, Azizan Ahmad <sup>2</sup> and Nor Sabirin Mohamed <sup>3,\*</sup>

<sup>1</sup> Institute of Graduate Studies, University of Malaya, 50603 Kuala Lumpur, Malaysia

<sup>2</sup> School of Chemical Sciences and Food Technology, Faculty of Science & Technology, Universiti Kebangsaan Malaysia, 46300 Bangi, Selangor, Malaysia; E-Mail: azizan@ukm.edu.my

<sup>3</sup> Center for Foundation Studies in Science, University of Malaya, 50603 Kuala Lumpur, Malaysia; E-Mail: nsabirin@um.edu.my

\* Author to whom correspondence should be addressed; E-Mail: nsabirin@um.edu.my or salmiah01@gmail.com; Tel.: +603-7967-5972.

Academic Editor: Christine Wandrey

Received: 15 January 2015 / Accepted: 10 April 2015 / Published: 16 April 2015

---

**Abstract:** Castor oil-based polyurethane as a renewable resource polymer has been synthesized for application as a host in polymer electrolyte for electrochemical devices. The polyurethane was added with LiI and NaI in different wt% to form a film of polymer electrolytes. The films were characterized by using attenuated total reflectance-Fourier transform infrared spectroscopy, dynamic mechanical analysis, electrochemical impedance spectroscopy, linear sweep voltammetry and transference number measurement. The highest conductivity of  $1.42 \times 10^{-6} \text{ S cm}^{-1}$  was achieved with the addition of 30 wt% LiI and  $4.28 \times 10^{-7} \text{ S cm}^{-1}$  upon addition of 30 wt% NaI at room temperature. The temperature dependence conductivity plot indicated that both systems obeyed Arrhenius law. The activation energy for the PU-LiI and PU-NaI systems were 0.13 and 0.22 eV. Glass transition temperature of the synthesized polyurethane decreased from  $-15.8 \text{ }^\circ\text{C}$  to  $\sim -26$  to  $-28 \text{ }^\circ\text{C}$  upon salts addition. These characterizations exhibited the castor oil-based polyurethane polymer electrolytes have potential to be used as alternative membrane for electrochemical devices.

**Keywords:** castor oil; polyol; polyurethane; polymer electrolytes

---

## 1. Introduction

Demands of developing polymeric conducting materials, which could be used in electrochemical devices, such as batteries, fuel cells, supercapacitor, electrochromic windows or photovoltaics, have increased research in polymer electrolytes extensively all over the world. However, the mass production of polymer electrolytes will bring environmental impact, because some polymers are non-degradable. Alternatively, research on developing biodegradable polymer electrolyte by using “environmental conscious” materials has become increasingly important with the aim to reduce environmental impact [1]. Kumar and Bhat [2] reported biodegradable synthetic polymer electrolytes based polyvinyl alcohol (PVA) for supercapacitor application. Pradeep and Shikha [3] appraised developments in the area of polymer electrolytes using aqueous and non-aqueous based natural polymers for developing cheaper, ecofriendly, biodegradable, and widely used electrolytes as substitutes for existing synthetic polymer electrolytes.

Recently, polyurethanes (PUs) have attracted attention as promising biodegradable polymer candidates for various applications [4–8]. Polyurethanes have many industrial applications due to a wide range of properties. The variation in properties of polyurethane is determined by several factors, such as the nature of the polyol and diisocyanate, the variation of hard segment concentration, the nature and ratios of the chain extenders, and density of chemical crosslinks [9–15]. Most previous research works focused on producing PU for application in coating for building and construction, transportation, furniture, bedding, *etc.* Only a few works were done on polymer electrolytes based on PU. However, the researchers used synthetic PUs [16–19]. PU has a unique multiphase structure, formed from soft and hard segments of the polymeric chain contributed by polyols and isocyanates, respectively. The soft segment acts as a polymeric solvent to solvate the cations and the hard segment responsible for dimensional stability acting as physical cross-link sites [20,21]. Furthermore, the low glass transition temperature,  $T_g$  and high segmental motion of polyether soft segments lead to higher mobility of the dissolved ions. The hard segment domains, which are in a glassy state and either distributed or interconnected throughout the rubbery phase of the soft segment, act as reinforcing filler and hence contribute to the dimensional stability of the polymer electrolytes [22].

Castor oil is one of the raw natural materials that can be used for producing PU. It is one of the most useful and economically important non-edible and non-volatile natural vegetable oil. It is also a unique industrial oil, due the presence of triglycerides of hydroxyl fatty acid known as ricinoleic acid. The ricinoleic acid content is about 87%–90%, which contains one hydroxyl group on the 12th carbon and double bond at the 9th and 10th carbons. It has hydroxyl functionality that is suitable in isocyanate reaction to make polyurethane elastomers [23,24]. These unique properties of castor oil make it useful for many polyurethane industries. For example, Somani *et al.* used castor oil-based PU as binders for surface coatings industries and for wood-to-wood bonding [25].

In this work, novel bio-polymer based electrolytes were synthesized from castor oil-polyol based PU and reacted with 4,4'-diphenylmethane diisocyanate (MDI) to form polyurethane as alternative renewable material for polymer electrolytes. Castor oil-polyol synthesized via transesterification reaction was used for the formation of bio-based polyurethane without using any chain extender. The castor oil-polyol possessed an OH value of 190 mg KOH/g, which was expected to obtain flexible PU. Furthermore, this type of polyurethane as host polymer applied in photoelectrochemical devices has

not yet been reported in the literature. The synthesized polyurethane was added with different wt% of lithium iodide and sodium iodide to form PU-LiI and PU-NaI electrolyte systems, respectively. Comparative analyses of the highest conducting PU-LiI and PU-NaI polymer films are presented in this article.

## 2. Experimental Section

### 2.1. Materials

Castor oil, glycerol (99.9%), acetone, potassium hydrogen phthalate, phthalate anhydride, potassium hydroxide (KOH), phenolphthalein and tetrahydrofuran (THF) were supplied by R&M (Marketing, Essex, UK). 4,4'-diphenylmethane diisocyanate was obtained from Merck (Hohenbrunn, Germany). Lithium iodide (LiI) and sodium iodide (NaI) were supplied by Sigma Aldrich (St. Louis, MO, USA). All the reagents were of analytical grade and used without further purification.

### 2.2. Synthesis of Castor Oil-Based Polyol and Polymer Electrolytes Preparation

Castor oil-based polyol were synthesized at ~200–220 °C in a four-necked round-bottom flask equipped with mechanical stirrer, thermometer, and nitrogen purge and modified condenser under constant stirring of ~200 rpm in the addition of glycerol and KOH as catalyst. After the formation of monoglyceride, the mixture was allowed to cool to 120 °C. Then the mixture was continuously stirring at ~200–220 °C after the addition of phthalate anhydride. The conversion to polyol was monitored by determining the acid value with respect to time. The acid value of the polyol was measured according to the American Society for Testing and Materials (ASTM) standards D 1639-90E 1. The hydroxyl value of the polyol was obtained using 848 Titrino Plus equipment (Metrohm, Riverview, FL, USA) and its value is 190 mg KOH/g. Castor oil-based polyurethane was formed upon addition of castor oil-polyol and MDI in the weight ratio of 80:20 (OH:NCO) and was confirmed by FTIR analysis.

Polymer electrolyte films of PU-LiI and PU-NaI were prepared by solution casting method. For the preparation of PU-LiI films, PU was dissolved in THF and 10% to 40 wt% of LiI were added to PU solution and stirred continuously for four hours (PU-10%LiI, PU-20%LiI, PU-30% LiI and PU-40% LiI). The homogeneous solutions were then cast in Teflon petri dishes and allow to evaporate at room temperature. The samples were kept in a desiccator filled with silica gel desiccants for further drying. The procedures were repeated for obtaining PU-NaI films.

### 2.3. Analytical Characterization

In order to study the formation of PU and interaction between the polymer and doping salt, Fourier transform infrared (FTIR) spectra were recorded using Perkin-Elmer (Waltham, MA, USA) Frontier spectrometer in the wavenumber range of 550–4000  $\text{cm}^{-1}$  at 2  $\text{cm}^{-1}$  resolution. Thermal characterizations of samples were executed with DMA 8000 Perkin Elmer dynamic mechanical analyzer (DMA) in film-tension mode at 1 Hz. Rectangular specimens of 20 mm  $\times$  10 mm  $\times$  0.60 mm (length  $\times$  thickness  $\times$  width) were used for the analysis. The samples were cooled and held isothermally at  $-60$  °C before the temperature was increased to 180 °C at a rate of 2 °C  $\cdot$  min $^{-1}$ . The glass transition temperatures,  $T_g$  of the samples were obtained from the peaks of the  $\tan \delta$  curves. Impedance measurements were done using

impedance spectroscopy using Solartron SI 1260 Impedance/Gain-Phase Analyzer (Solartron, Hampshire, UK). The measurements were performed over frequency range of 10 Hz–5 MHz with applied voltage of amplitude of 100 mV from room temperature to 363 K. All samples were sandwiched by two polished stainless steel blocking electrodes. The values of bulk resistance,  $R_b$  of the electrolytes were determined from the Nyquist plots obtained. Conductivity,  $\sigma$  values were calculated using equation:

$$\sigma = \frac{t}{R_b A} \quad (1)$$

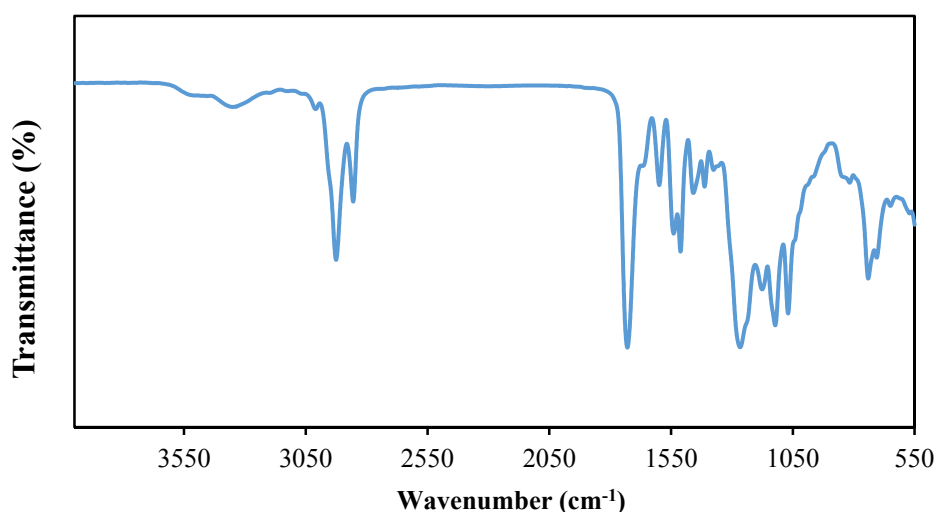
where  $t$  is the thickness of the electrolyte and  $A$  is the electrolyte-electrode contact area.

For ionic transference number measurement, stainless steel (SS) blocking electrodes were used and the polymer electrolytes were polarized under a fixed direct current (DC) voltage of 1.0 V. The ionic ( $t_{ion}$ ) and electronic transference numbers ( $t_{electron}$ ) were evaluated by means of Wagner's polarization technique. The linear sweep voltammetry was performed for the SS/polymer electrolytes/SS cell in the potential range of  $-2.5$  to  $4.0$  V with a scan rate of  $0.5 \text{ mV} \cdot \text{s}^{-1}$ .

### 3. Results and Discussion

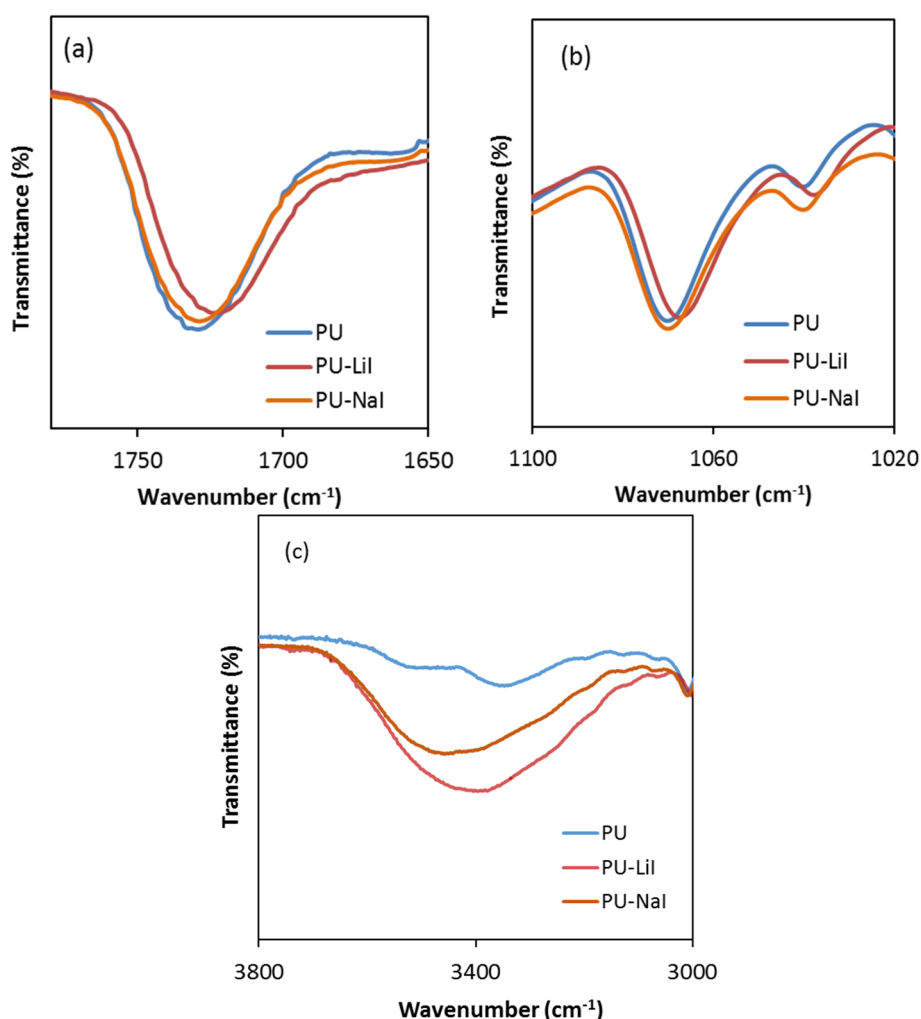
#### 3.1. Fourier Transform Infrared Spectroscopy

The Fourier transform infrared spectrum of castor oil-based PU is shown in Figure 1. The absence of the band in the  $2260$  to  $2310 \text{ cm}^{-1}$  range confirms the absence of free NCO group in the polymer structure, which indicates the completion of the urethane reaction. The most important characteristic features of the PU are the presence of bands at  $1072 \text{ cm}^{-1}$  (C–N stretching vibrations),  $1123 \text{ cm}^{-1}$  (C–O stretching vibrations),  $1557$ – $1580 \text{ cm}^{-1}$  (C–N stretching and N–H bending),  $1600 \text{ cm}^{-1}$  (C–C stretching vibration),  $1720$ – $1730 \text{ cm}^{-1}$  (C–O stretching vibrations from urethane groups),  $2857$ – $2925 \text{ cm}^{-1}$  ( $\text{CH}_2$  symmetric and anti-symmetric stretching vibrations) and  $3378 \text{ cm}^{-1}$  (free O–H and N–H stretching from urethane group stretching vibrations). These vibrational bands show the formation of urethane linkage, NH–COO in the synthesized polyurethane [26,27].



**Figure 1.** FTIR spectrum of castor oil-based polyurethane.

Figure 2 illustrates the vibrational regions of carbonyl, ether, ester and amine functional groups in polyurethane-salt complexes. The foremost interests in the PU polymer electrolytes are on the oxygen atoms of the carbonyl (C=O) ( $1750\text{--}1710\text{ cm}^{-1}$ ), ether and ester group (C–O–C) ( $1300\text{--}1000\text{ cm}^{-1}$ ) and amine functional groups (C–N and N–H) ( $1550\text{--}1500\text{ cm}^{-1}$ ) [28]. According to Chen *et al* [29], the convoluted FTIR spectra in the C=O stretching region have three peaks due to free or non-hydrogen-bonded C=O ( $1727\text{--}1735\text{ cm}^{-1}$ ), disordered hydrogen-bonded C=O ( $1718\text{--}1721\text{ cm}^{-1}$ ) and ordered hydrogen bonded C=O ( $1703\text{--}1704\text{ cm}^{-1}$ ) vibrations, respectively. The disordered hydrogen-bonded C=O corresponds to the hydrogen-bonding interactions with –NH groups in both amorphous and crystalline regions, whereas the ordered hydrogen-bonded C=O occurs within the crystalline hard domain of the PU [30].



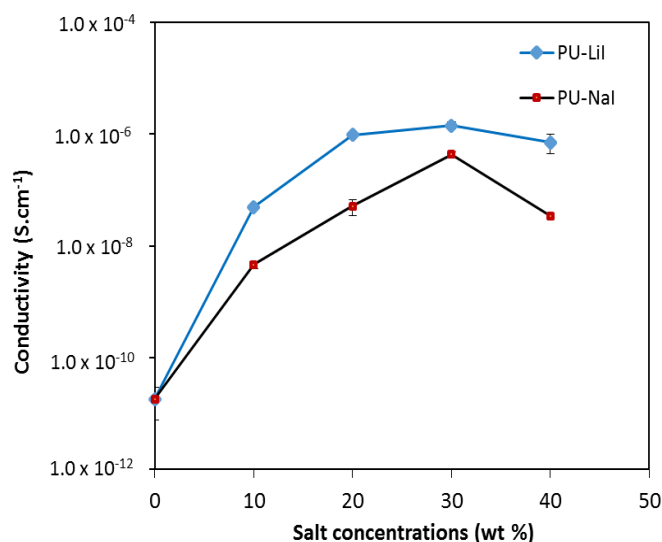
**Figure 2.** FTIR spectra in (a) C=O and (b) C–O–C and (c) NH vibrational regions.

Figure 2a shows FTIR spectra in the region of PU and polymer-salt complexes. The band of C=O functional group is shifted to lower wavenumbers of  $1732\text{ to }1730\text{ cm}^{-1}$  and  $1726\text{ cm}^{-1}$  upon the addition of lithium and sodium iodide salts, respectively. These changes indicate that the C=O region is affected by the introduction of salts, possibly because of the coordination of  $\text{Li}^+$  and  $\text{Na}^+$  ions with carbonyl oxygen atoms. This shifting also indicates the existences of strong intermolecular interaction between lithium and sodium ions and oxygen atoms in the polymer. The oxygen atoms from carbonyl functional group in the PU act as electron donor atoms and hence form a coordinate bond with lithium and sodium

ions from doping salts. The peak  $1072\text{ cm}^{-1}$  due to ether group (C–O–C) shifted to  $1070\text{ cm}^{-1}$  with the addition of sodium iodide and  $1068\text{ cm}^{-1}$  with the addition of lithium iodide salt, (Figure 2b). Figure 2c exhibits the N–H peak of PU at  $3370\text{ cm}^{-1}$  shifted to a higher wavenumber with the addition of salts. It could be explained on the basis of interaction of  $\text{Li}^+$  and  $\text{Na}^+$  ions with the N atoms of free –NH groups. Interaction of cation with the lone pair of electrons on the N atom leads to weakening of the N–H bond length. It is also could be due to interaction of the cations to the nonbonded electrons of the carbonyl oxygen atoms that leads to reducing the H-bond strength [31,32]. From these FTIR results, it can be deduced that the interactions between host polymer and salts occurred both in the hard segment (C=O and N–H) and soft segment (C–O–C) of PU.

### 3.2. Room Temperature Conductivity

The plots of room temperature conductivity of polymer electrolytes as a function of salt concentration are shown in Figure 3. The conductivity of both systems increases with the salt concentrations, reaching a maximum values of  $1.78 \times 10^{-6}$  and  $4.28 \times 10^{-7}\text{ S}\cdot\text{cm}^{-1}$  at 30 wt% of LiI and NaI, respectively, and decreases thereafter. The conductivity increase is due to the increase in charge carriers or mobile ions when the salt content increases. At high salt concentration, the distance between dissociated ions became too close to each other enabling them to recombine into neutral ion-pairs and do not contribute to conductivity. Such phenomenon has also been reported in the literature [17,33,34]. By comparing the systems containing LiI and NaI, the conductivity is higher for PU-LiI compared to that for PU-NaI due to the size of cations. The cation size of  $\text{Li}^+$  and  $\text{Na}^+$  are 0.76 and 1.02 Å, respectively [35]. According to Bhattacharya *et al.* [35] systems containing salt with smaller cations exhibit higher conductivity due to higher mobility of the cation.



**Figure 3.** Conductivity of PU based polymer electrolytes with different wt% of LiI and NaI.

The conductivity values obtained in this work are comparable with that reported by Huh *et al* [34], which is  $2.6 \times 10^{-6}\text{ S}\cdot\text{cm}^{-1}$  using synthetic PU based polymer electrolytes in solid-state form. The conductivity is quite low and expected to be increased with addition of plasticizers or ionic liquid [36,37]. According to Minami *et al* [38], ionic conductivity in solid polymer electrolytes based on

polyether complexed with salt is lower compared to other polymers. This might be due to the low degree of dissociation of salt leads to low concentration of carrier ions and strong interaction between cations and electrons donor atoms of the polymer chains. However, the polymer electrolytes are flexible and therefore can easily make good contact with electrode materials and thus are suitable for application in electrochemical devices.

### 3.3. Temperature Dependent Conductivity

The temperature-dependent ionic conductivity measurements for the highest conducting PU-LiI and PU-NaI were carried out to analyze the mechanism of ionic conduction in the polymer electrolytes. Displayed in Figure 4 is the variation of ionic conductivity with reciprocal of temperature for the PU-LiI and PU-NaI polymer electrolytes. The regression values for both plots are 0.998 for PU-LiI and 0.990 for PU-NaI indicating that the points lie in almost straight line. The conductivity increases linearly with the increase of temperature. The linear variation of  $\log \sigma$  versus  $1000/T$  plots suggests an Arrhenius-type thermally activated process. This means that as temperature increases, the polymer chain acquires faster internal modes in which bond rotations produce segmental motion. This, in turn, favors hopping inter-chain and intra-chain ion movements and, accordingly, the conductivity of the polymer electrolytes becomes higher [39,40]. The Arrhenian conductivity-temperature relationship has also been observed for systems of polyurethane acrylates-LiClO<sub>4</sub> [41]. Arrhenius equation is expressed as:

$$\sigma = \sigma_0 \exp\left(\frac{-E_a}{K_b T}\right) \quad (2)$$

where  $\sigma_0$  is a pre-exponential factor,  $E_a$  is the activation energy,  $T$  is the absolute temperature in Kelvin and  $K_b$  is Boltzman constant ( $8.6173324 \times 10^{-5}$  eV·K<sup>-1</sup>). The activation energy values were calculated from the slope of  $\log \sigma$  versus  $1000/T$  graph. The  $E_a$  for PU-LiI electrolytes is found to be 0.13 eV. Meanwhile the  $E_a$  for PU-NaI is 0.22 eV. The value of activation energy is lower for the system with high ionic conductivity and vice versa indicated that the higher conducting electrolytes require only a smaller amount of energy to start a migration process.

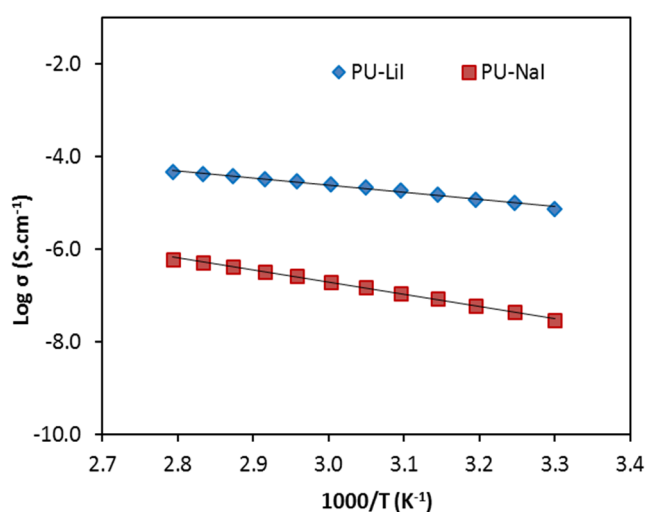


**Figure 4.** Temperature dependence of ionic conductivity of PU-LiI and PU-NaI polymer electrolytes.

### 3.4. Dynamic Mechanical Analysis

Dynamic mechanical analysis was performed in order to determine glass transition temperature of the synthesized PU and polymer electrolytes. Figure 5 presents the storage modulus and tangent delta as functions of temperature for the studied PU polymer electrolyte films. At very low temperatures, the polymer is in glassy state and the modulus almost remains constant until a critical temperature corresponding to the start of energy dissipation and cooperative chain motions. Figure 5a shows as temperature increases from  $-60$  °C, storage modulus  $E'$  slightly decreases, and once  $-40$  °C is reached, a rapid decrease in  $E'$  is observed. This change is corresponding to the glass-rubber transition and  $\tan\delta$  reaches its maximum peak simultaneously (Figure 5b). The magnitude of storage modulus decreased with temperature for all samples because the materials become more amorphous when heated, therefore capacity for energy absorption is diminished [24]. A rubbery plateau for the storage modulus is observed in the higher temperature range. By comparing PU and PU electrolyte films, PU electrolyte films have higher magnitude value of storage modulus in the rubbery region due to the presence of salts in the systems. This reflects to the good mechanical properties of the films [42].

The peak maximum ( $\alpha$  relaxation) in the plot of  $\tan\delta$  versus temperature, Figure 5b is identified as glass transition temperature,  $T_g$  of materials. The figure shows the  $T_g$  of polyurethane film of  $-15.8$  °C decreases to  $-27.5$  °C and  $-26.1$  °C upon the addition of LiI and NaI, respectively. An electrolyte with low  $T_g$  implies fast ion conduction. This agree well with conductivity result which shows that PU-LiI electrolytes has higher conductivity than PU-NaI electrolytes. The shift of  $T_g$  value towards lower temperature suggests that the segmental mobility of PU increases upon the addition of salts and the segment become less rigid. It is also could be due to the plasticization of the electrolyte with the addition of salts. The incorporation of the salt into the PU matrix results in weakening of the dipole-dipole interactions between the PU chains, which makes the ions move freely through the polymer chain network when an electric field is applied and hence increase the conductivity.

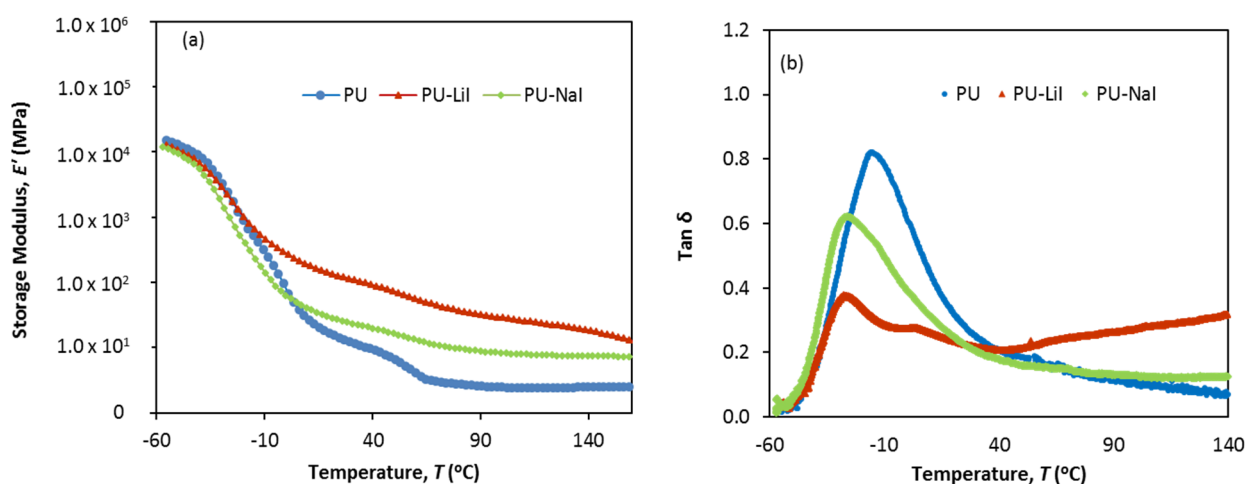


**Figure 5.** (a) Storage modulus,  $E'$  and (b)  $\tan\delta$  as a function of temperature of PU, PU-LiI and PU-NaI polymer electrolytes.

### 3.5. Electrochemical Studies

The electrochemical stability window of PU electrolytes was determined by linear sweep voltammetry [43]. Figure 6 displays the current-voltage response obtained for both polymer electrolyte systems using stainless steel as a working electrode and reference electrode measured between the potential ranges from  $-2.5$  to  $4.5$  V with a scan rate of  $0.5 \text{ mV} \cdot \text{s}^{-1}$ . The onset of the current identifies the anodic decomposition voltage of the electrolytes [44]. It is observed that PU-NaI shows decomposition voltage at  $1.8$  V, whereas for PU-LiI, the decomposition voltage is  $2.0$  V. The results show that the PU-LiI is slightly electrochemically stable compared to PU-NaI.

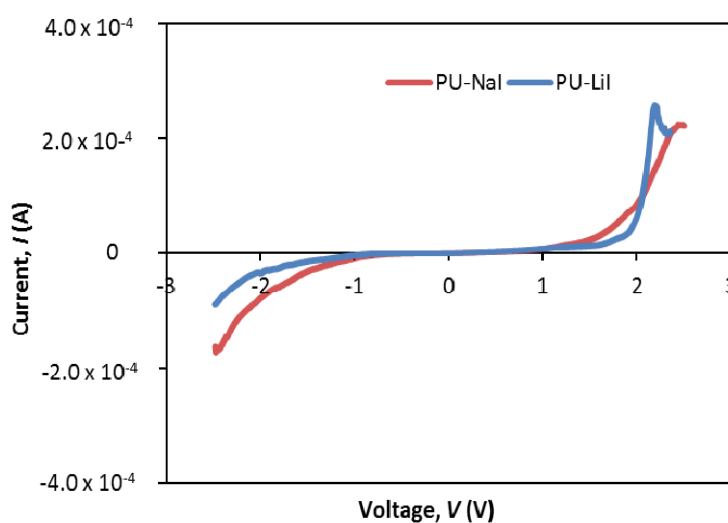


**Figure 6.** Linear sweep voltammograms of PU-LiI and PU-NaI polymer electrolyte systems.

### 3.6. Transference Number Measurement

Using Wagner's polarization technique, transference numbers corresponding to ionic ( $t_{\text{ion}}$ ) and electronic ( $t_{\text{electron}}$ ) were estimated for PU-LiI and PU-NaI electrolyte systems. In this method, the DC current is observed as a function of time on application of a fixed voltage across the SS/Polymer electrolyte/SS cell. The normalized current *versus* time plots of the polymer electrolytes are shown in Figure 7. The ionic and electronic transference numbers are estimated using equations:

$$t_{\text{ion}} = \frac{I_1 - I_f}{I_1} \quad (3)$$

$$t_{\text{ele}} = \frac{I_f}{I_1}$$

where  $I_1$  is the initial current and  $I_f$  is the final residual current [45]. The values of transference number are 0.99 to 0.98 for the PU-LiI and PU-NaI, respectively. This suggests that the charge transport in these polymer electrolyte films is predominantly due to ions and only small contributions from electrons.

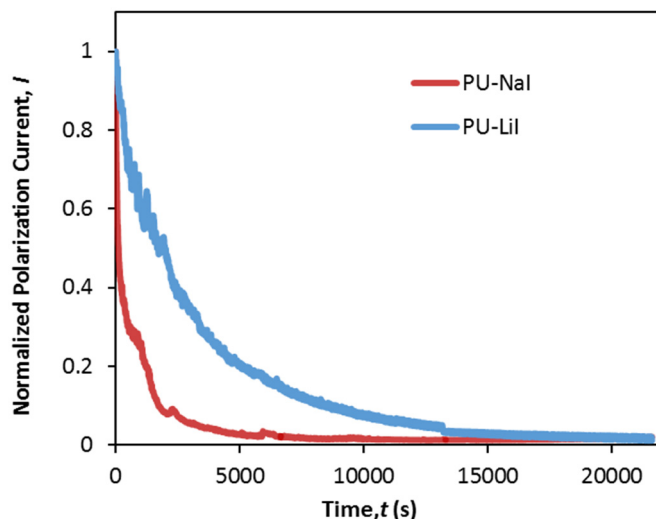


**Figure 7.** The plots of normalized polarization current with time for PU-LiI and PU-NaI polymer electrolytes.

#### 4. Conclusions

Castor oil-based PU was successfully synthesized and confirmed by FTIR result. The interaction of synthesized PU with LiI and NaI salts is indicated by the shifting of wavenumbers of C=O, C–O–C and N–H groups. PU based polymer electrolytes containing LiI showed higher ionic conductivity than PU based polymer electrolytes containing NaI. Both systems showed an increase in ionic conductivity up to 30 wt% of salts, which was attributed to the enhancement in the number of charge carriers. The ionic conductivity decreased for higher salt contents. It is probably due to retarding effect of ion aggregates acting as the barrier for the ionic movement. DMA results showed a decrease in  $T_g$  value of PU upon addition of salts due to plasticization effect that lead to weakening the dipole-dipole interaction between the PU chains. Electrochemical stability window of the castor oil-based PU polymer electrolytes was stable up to 2.0 and 1.8 V for PU-LiI and PU-NaI, respectively, as determined from the onset of current in linear sweep voltammograms. The result of transference number measurement for both polymer electrolyte systems confirmed the ionic transport in the systems. These results showed castor oil polyurethane could be used as alternative bio based polymer membrane in polymer electrolytes.

#### Acknowledgments

The authors are grateful to the University of Malaya for financial support under Postgraduate Research Fund, Grant No. PG073/2012B. A highly gratitude goes to the Ministry of Education, Malaysia for the scholarship under the Graduate Scheme Program MyBrain15 given to Salmiah Ibrahim.

#### Author Contributions

All listed authors contributed to the research work. Nor Sabirin Mohamed conceived and directed the research, Salmiah Ibrahim conducted, analyzed and interpreted the data. Azizan Ahmad and Nor Sabirin Mohamed proposed idea for explanation, reviewed and approved the manuscript.

## Conflicts of Interest

The authors declare no conflict of interest.

## References

1. Fonseca, C.P.; Rosa, D.S.; Gaboardi, F.; Neves, S. Development of a biodegradable polymer electrolyte for rechargeable batteries. *J. Power Sources* **2006**, *155*, 381–384.
2. Kumar, M.S.; Bhat, D.K. Polyvinyl alcohol-polystyrene sulphonic acid blend electrolyte for supercapacitor application. *Phys. B* **2009**, *404*, 1143–1174.
3. Pradeep, K.V.; Shikha, G. Natural polymer-based electrolytes for electrochemical devices: Review. *Ionics* **2011**, *17*, 479–483.
4. Meier, M.A.R.; Metzger, J.O.; Schubert, U.S. Plant oil renewable resources as green alternatives in polymer science. *Chem. Soc. Rev.* **2007**, *36*, 1788–1802.
5. Cateto, C.A.; Barreiro, M.F.; Rodrigues, A.E. Monitoring of lignin-based polyurethane synthesis by FTIR-ATR. *Ind. Crop. Prod.* **2008**, *27*, 168–174.
6. Lee, H.-S.; Han, C.-H.; Sung, Y.-M.; Sekhon, S.S.; Kim, K.-J. Gel electrolyte based on UV-cured polyurethane for dye-sensitized solar cells. *Curr. Appl. Phys.* **2011**, *11*, S158–S162.
7. Rashmi, B.J.; Rusu, D.; Prashantha, K.; Lacrampe, M.F.; Krawczak, P. Development of water-blown bio-based thermoplastic polyurethane foams using bio-derived chain extender. *J. Appl. Polym. Sci.* **2013**, *128*, 292–303.
8. Datta, J.; Głowińska, E. Chemical modifications of natural oils and examples of their usage for polyurethane synthesis. *J. Elastom. Plast.* **2012**, doi: 10.1177/0095244312459282.
9. Liao, L.; Cao, Q.; Liao, H. Investigation of a hyperbranched polyurethane as a solid-state phase change material. *J. Mater. Sci.* **2010**, *45*, 2436–2441.
10. Bil, M.; Ryszkowska, J.; Kurzydłowski, K.J. Effect of polyurethane composition and the fabrication process on scaffold properties. *J. Mater. Sci.* **2009**, *44*, 1469–1476.
11. Oprea, S. Dependence of fungal biodegradation of PEG/castor oil-based polyurethane elastomers on the hard-segment structure. *Polym. Degrad. Stab.* **2010**, *95*, 2396–2404.
12. Da Silva, G.R.; da Silva-Cunha, A., Jr.; Vieira, L.C.; Silva, L.M.; Ayres, E.; Oréfice, R.L.; Fialho, S.L.; Saliba, J.B.; Behar-Cohen, F. Montmorillonite clay based polyurethane nanocomposite as substrate for retinal pigment epithelial cell growth. *J. Mater. Sci. Mater. Med.* **2013**, *24*, 1309–1317.
13. Oprea, S. Effect of the long chain extender on the properties of linear and castor oil cross-linked PEG-based polyurethane elastomers. *J. Mater. Sci.* **2011**, *46*, 2251–2258.
14. Datta, J.; Kacprzyk, M. Thermal analysis and static strength of polyurethanes obtained from glycolysates. *J. Therm. Anal. Calorim.* **2008**, *93*, 753–757.
15. Datta, J. Synthesis and investigation of glycolysates and obtained polyurethane elastomers. *J. Elastom. Plast.* **2010**, *42*, 117–127.
16. Santhosh, P.; Vasudevan, T.; Gopalan, A.; Lee, K.-P. Preparation and properties of new cross-linked polyurethane acrylate electrolytes for lithium batteries. *J. Power Sources* **2006**, *160*, 609–620.
17. Wu, F.; Li, Y.J.; Chen, R.J.; Chen, S. Preparation and characterization of a mixing soft-segment waterborne polyurethane polymer electrolyte. *Chin. Chem. Lett.* **2009**, *20*, 115–118.

18. Lavall, R.L.; Ferrari, S.; Tomasi, C.; Marzantowicz, M.; Quartarone, E.; Fagnoni, M.; Mustarelli, P.; Saladino, M.L. MCM-41 silica effect on gel polymer electrolytes based on thermoplastic polyurethane. *Electrochim. Acta* **2012**, *60*, 359–365.
19. Leszkowski, K.; Haponiuk, J.; Datta, J. Preparation and properties of ion conductive polyurethane materials. *Przem. Chem.* **2012**, *91*, 1999–2002.
20. Su'ait, M.S.; Ahmad, A.; Badri, K.H.; Mohamed, N.S.; Rahman, M.Y.A.; Azanza Ricardo, C.L.; Scardi, P. The potential of polyurethane bio-based solid polymer electrolyte for photoelectrochemical cell application. *Int. J. Hydrog. Energy* **2014**, *39*, 3005–3017.
21. Wang, S.; Min K. Solid polymer electrolytes of blends of polyurethane and polyether modified polysiloxane and their ionic conductivity. *Polymer* **2010**, *51*, 2621–2528.
22. Santhosh, P.; Gopalan, A.; Vasudevan, T.; Lee, K.-P. Evaluation of a cross-linked polyurethane acrylate as polymer electrolyte for lithium batteries. *Mater. Res. Bull.* **2006**, *41*, 1023–1037.
23. Petrovic, Z.S. Polyurethanes from vegetable oils. *Polym. Rev.* **2008**, *48*, 109–155.
24. Jiménez, M.A.G.; Armenta, J.L.R.; Martínez, A.M.M.; Muñiz, R.; Vazquez, N.A.R.; Rojas, E.T. Interpenetrating polymer networks based on castor oil polyurethane/cellulose derivatives and polyacrylic acid. *Lat. Am. Appl. Res.* **2009**, *39*, 131–136.
25. Somani, K.P.; Kansara, S.S.; Patel, N.K.; Rakshit, A.K. Castor oil based polyurethane adhesives for wood-to-wood bonding. *Int. J. Adhes. Adhes.* **2003**, *23*, 269–275.
26. Jena, K.K.; Chattopadhyay, D.K.; Raju, K.V.S.N. Synthesis and characterization of hyperbranched polyurethane-urea coatings. *Eur. Polym. J.* **2007**, *43*, 1825–1837.
27. Thakur, S.; Karak, N. Castor oil-based hyperbranched polyurethanes as advanced surface coating materials. *Prog. Org. Coat.* **2013**, *76*, 157–164.
28. Pavia, D.L.; Lampman, G.M.; Kriz, G.S.; Vyvyan, J.R. *Introduction to Spectroscopy*, 4th ed.; Cengage Learning: Boston, MA, USA, 2008.
29. Chen, W.-C.; Chen, H.-H.; Wen, T.-C.; Digar, M.; Gopalan, A. Morphology and ionic conductivity of thermoplastic polyurethane electrolytes. *J. Appl. Polym. Sci.* **2004**, *91*, 1154–1167.
30. Van Heumen, J.D.; Stevens, J.R. The role of lithium salts in the conductivity and phase morphology of a thermoplastic polyurethane. *Macromolecules* **1995**, *28*, 4268–4277.
31. Wen, T.-C.; Du, Y.-L.; Digar, M. Compositional effect on the morphology and ionic conductivity of thermoplastic polyurethane based electrolytes. *Eur. Polym. J.* **2002**, *38*, 1039–1048.
32. Yang, C.-H.; Lin, W.-C.; Liu, F.-J. Waterborne polyurethane single-ion electrolyte from aliphatic diisocyanate and various molecular length of polyethylene glycol. *Express Polym. Lett.* **2007**, *1*, 142–149.
33. Rodrigues, L.C.; Barbosa, P.C.; Silva, M.M.; Smith, M.J. Electrochemical and thermal properties of polymer electrolytes based on poly(epichlorohydrin-co-ethylene oxide-co-ally glycidyl ether). *Electrochim. Acta* **2007**, *53*, 1427–1431.
34. Huh, P.-H.; Choi, M.-G.; Jo, N.J.; Lee, J.-K.; Lee, J.-O. Effect of salt concentration on the glass transition temperature and ionic conductivity of poly(ethylene glycol)-polyurethane/LiClO<sub>4</sub> complexes. *Macromol. Res.* **2004**, *12*, 422–426.
35. Bhattacharya, B.; Lee, J.Y.; Geng, J.; Jung, H.-T.; Park, J.-K. Effect of cation size on solid polymer electrolyte based dye-sensitized solar cells. *Langmuir* **2009**, *25*, 3276–3281.

36. Lavall, R.L.; Ferrari, S.; Tomasi, C.; Marzantowicz, M.; Quartarone, E.; Magistris, A.; Mustarelli, P.; Lazzaroni, S.; Fagnoni, M. Novel polymer electrolytes based on thermoplastic polyurethane and ionic liquid/lithium bis(trifluoromethanesulfonyl) imide/propylene carbonate salt system. *J. Power Sources* **2010**, *195*, 5761–5767.
37. Gao, R.; Zhang, M.; Wang, S.W.; Moore, R.B.; Colby, R.H.; Long, T.E. Polyurethanes containing an imidazolium diol-based ionic-liquid chain extender for incorporation of ionic-liquid electrolytes. *Macromol. Chem. Phys.* **2013**, *214*, 1027–1036.
38. Minami, T.; Tatsumisago, M.; Wakihara, M.; Iwakura, C.; Kohjiya, S.; Tanaka, I. *Solid State Ionics for Batteries*; Springer Science and Business Media: New York, NY, USA, 2005; p. 104.
39. Baskaran, R.; Selvasekarapandian, S.; Kuwata, N.; Kawamura, J.; Hattori, T. Conductivity and thermal studies of blend polymer electrolytes based on PVAC-PMMA. *Solid State Ion.* **2006**, *177*, 2679–2682.
40. Reddy, C.V.S.; Sharma, A.K.; Rao, V.V.R.N. Conductivity and discharge characteristics of polyblend (PVP + PVA + KIO<sub>3</sub>) electrolyte. *J. Power Sources* **2003**, *114*, 338–345.
41. Ren, T.; Huang, X.; Zhao, X.; Tang, X. The effects of salt concentration on ion state and conductivity in comb cross-linked polymer electrolytes. *J. Mater. Sci.* **2003**, *38*, 3007–2011.
42. Samir, M.A.S.A.; Alloin, F.; Sanchez, J.-Y.; Dufresne, A. Cross-linked nanocomposite polymer electrolytes reinforced with cellulose whiskers. *Macromolecules* **2004**, *37*, 4839–4844.
43. Appetecchi, G.B.; Croce, F.; Scrosati, B. High-performance electrolyte membranes for plastic lithium batteries. *J. Power Sources* **1997**, *66*, 77–82.
44. Deka, M.; Kumar, A.; Deka, H.; Karak, N. Ionic transport studies in hyperbranched polyurethane/clay nanocomposite gel polymer electrolytes. *Ionics* **2011**, *18*, 181–187.
45. Sreekanth, T.; Reddy, M.J.; Ramalingaiah, S.; Subba Rao, U.V. Ion-conducting polymer electrolyte based on polyethylene oxide/complexed with NaNO<sub>3</sub> salt-application as an electrochemical cell. *J. Power Sources* **1999**, *79*, 105–110.

© 2015 by the authors; licensee MDPI, Basel, Switzerland. This article is an open access article distributed under the terms and conditions of the Creative Commons Attribution license (<http://creativecommons.org/licenses/by/4.0/>).